Optics & Laser Technology 44 (2012) 337–340

Contents lists available at ScienceDirect

Optics & Laser Technology

journal homepage: www.elsevier.com/locate/optlastec

Investigation of optical photorefractive properties of Zr:Fe:$LiNbO_3$ crystals

Zifan Zhou [a,b,*], Biao Wang [a,**], Shaopeng Lin [a], Yilun Li [a], Kun Wang [a]

[a] School Physical Science and Engineering, No. 135, West Xingang Road, Sun Yat-Sen University, Guangzhou 510275, China
[b] College of Science, Foshan University, Foshan 528000, China

ARTICLE INFO

Article history:
Received 1 August 2010
Received in revised form
5 July 2011
Accepted 14 July 2011
Available online 24 August 2011

Keywords:
Zr:Fe:$LiNbO_3$
Optical damage
Holographic properties

ABSTRACT

A series of Zr:Fe:$LiNbO_3$ crystals with various levels of ZrO_2 doping were grown by Czochraski technique. The optical damage resistance and photorefractive properties were deeply explored. The results showed that the ability optical damage resistance increased remarkably when the concentration of ZrO_2 is over threshold concentration, but which is lower than that of traditional damage resistant additive MgO. While, the holographic storage properties can be greatly enhanced by proper level of ZrO_2 doping in Fe:$LiNbO_3$. In terms of ions' site occupation model, the photo-damage resistant ability enhancement and the change of the photorefractive properties were discussed.

1. Introduction

The $LiNbO_3$ crystal is one of the most widely used electro-optical materials. One of the important applications is holographic storage because of its excellent photorefractive properties. However, the applications are severely limited by optical damage, which induces birefringence change at high laser intensities [1]. Doping with damage resistant additive is found to be an effective method to increase the optical damage resistance [2]. Some damage resistant elements, such as Mg [3], Zn [4], In [5], Sc [6], Hf [7–10] and Zr [11–15] have been used to decrease the optical damage of $LiNbO_3$ crystals. It has been known that there exist threshold concentrations for these damage resistant additives. When the doping concentrations are above the threshold values, response speed and photorefractive sensitivity are remarkably improved, nevertheless diffraction efficiency will apparently decrease. Hf [7] was reported improving the optical damage ability and keeping high diffraction efficiency. Zr as a tetravalent ion was studied by lot of researchers. While different results have been got, such as the threshold concentration was 1.7(mol%) in Kong et al.'s result [11], Sun et al.'s [12] result was 4–6 (mol%), great different optical damage resistance ability existed too.

In this work, ZrO_2 damage resistant additive was employed to enhance the optical damage resistance. Different threshold concentration was obtained and the optical damage resistance ability was accurately measured. The correlation between defects and optical properties of these crystals were explored and the rational explanation of were given.

2. Experimental procedures

2.1. Samples preparation

We carried out experiments for four samples of $LiNbO_3$, three of them doped by iron and zirconium (Zr:Fe:$LiNbO_3$). Various factors affecting the control of crystal growth and the relationship among these factors were analyzed, and an auto-monitoring and adjusting diameter-constant control system was built up. Using this control system, various levels of ZrO_2 doping crystals were successfully grown. These crystals show smooth surface from shoulder, body to tail .One of the crystals was shown in Fig. 1.

The bulk doped crystals were grown from a congruent melt of Li/Nb=48.6/51.4 by Czochraski technique. The specimens were doped by iron at fixed mass concentration 0.15 wt% and by zirconium at various molar concentrations 0, 2, 4 and 5 mol%, which we referred to as Zr0, Zr2, Zr4 and Zr5, respectively. The raw material compositions of the samples in the melt were shown in Table 1.

In order to form polycrystalline bulk, the raw materials, which had been precisely weighed and thoroughly mixed for 24 h, were fully calcined at 750 °C for 2 h and then sintered at 1150 °C for 2 h. The crystals were grown under the optimum technology conditions: temperature gradient of 40–50 °C cm^{-1} along the furnace axial direction, rotating rate of 15–25 rpm and pulling rate of 1.2–2.0 mm h^{-1}. The typical as-grown crystal sizes were about 25–35 mm in diameter and 40 mm in length.

* Corresponding author at: School Physical Science and Engineering, No. 135, West Xingang Road, Sun Yat-Sen University, Guangzhou 510275, China.
** Corresponding author.
E-mail address: zzf0511@sina.com (Z. Zhou).

0030-3992/$ - see front matter © 2011 Elsevier Ltd. All rights reserved.
doi:10.1016/j.optlastec.2011.07.010

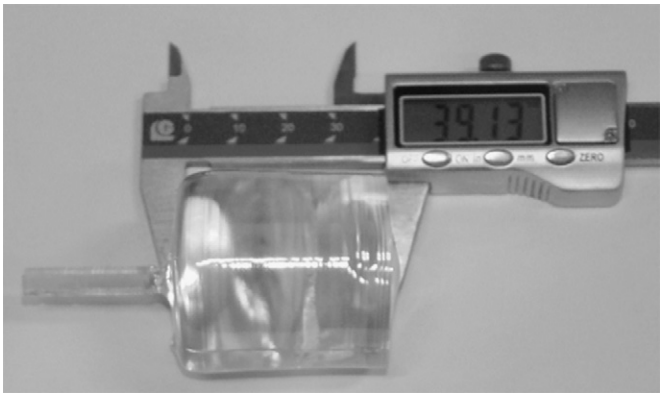

Fig. 1. As-grown crystal.

Table 1
Doped Zr:FeLiNbO$_3$ Crystal samples in experiment.

Crystals	Composition	Dopant in starting melt
Zr0	Fe:LiNbO$_3$	0.015 wt% Fe_2O_3
Zr2	Zr:Fe:LiNbO$_3$	2 mol%ZrO_2, 0.015 wt% Fe_2O_3
Zr4	Zr:Fe:LiNbO$_3$	4 mol%ZrO_2, 0.015 wt% Fe_2O_3
Zr5	Zr:Fe:LiNbO$_3$	5 mol%ZrO_2, 0.015 wt% Fe_2O_3

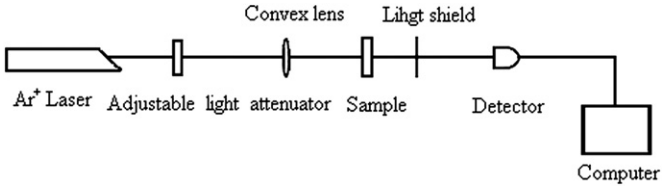

Fig. 2. Experimental set-up fo r measuring the light-induced scattering.

2.2. Measurements

The infrared transmission spectra of the crystals were obtained with a Fourier infrared spectrophotometer in the 3000–4000 cm^{-1} wave number range at room temperature.

The optical damage resistance of the crystals was characterized by measuring the light-induced scattering intensity change as a function of the incident light intensity. As shown in Fig. 2, an argon-ion laser was used as light source, and the incident beam power level could be adjusted by an attenuator. The crystal *c* axis was set parallel to the polarization direction of the laser beam and placed on the back focal plane of the convex lens. The power density of the beam spot passing through a pin hole on a light shield was measured by a photodiode connected with a computer. The light-induced scattering light intensity $I_s=I_0-I_1$, where I_0 is the transmitted light intensity just at the beginning and I_1 is the transmitted light intensity at saturation. $R=I_s/I_0$ is defined as the strength of light-induced scattering.

The holographic properties were investigated by two wave-mixing in transmission geometry at a fixed grating spacing (as shown in Fig. 3) at room temperature. Two mutually coherent and extraordinarily polarized green beams from a doubled Nd:YAG laser ($\lambda=532$ nm) were used as writing beams, i.e. signal beam S and reference beam R. The grating vector of written holograms was aligned along the *c* axis to utilize the largest electro-optic coefficient γ_{33}, and the crossing angle between the wring beams was $\sim 20^\circ$ in air with a grating period of 1.2 um. The R–S intensity was adjusted by rotation of half-wave plate HW_1 to be equal (150 mW cm^{-2}).

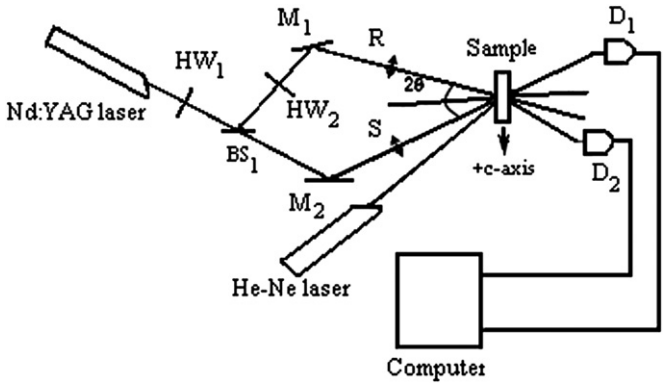

Fig. 3. Experimental set-up for two-wave coupling. M_1, M_2: mirrors; BS_1: beam splitter; D_1, D_2: detectors; R: reference beam; S: signal beam; HW_1, HW_2: half-wave plates.

The measured diffraction efficiency η was defined as $I_d/(I_d+I_t)$, where I_d and I_t are the diffracted and transmitted intensity of the read out beam, respectively. After the diffraction efficiency had reached its maximum value, the signal beam was blocked, and the hologram was read out with the reference beam and the recorded grating decayed gradually due to beam erasure. Meanwhile, I_t and I_d of probe laser beam were also detected to record the erasure process. The behavior of the grating formation and erasure can be approximately described by the relations:

$$\eta_{gf}^{1/2}=\eta_s^{1/2}\left[1-\exp\left(-\frac{\tau}{\tau_t}\right)\right] \tag{1}$$

$$\eta_{ef}^{1/2}=\eta_s^{1/2}\left[\exp\left(-\frac{\tau}{\tau_e}\right)\right] \tag{2}$$

where τ_t and τ_e are the response time and the erasure time, respectively, and η_s is the saturated value of diffraction efficiency. Fitting the experimental data of diffraction efficiency versus time to the above two expressions, the response time τ_r and the erasure time τ_e can be estimated. Thus, the photoconductivity can also be obtained by $\sigma_{ph}=\varepsilon\varepsilon_0/\tau_e$, where ε is the relative dielectric constant and ε_0 is the dielectric constant of vacuum. As metrics for hologram storage, two figures of merit are also used: photorefractive sensitivity *S* and dynamic range *M*/#. They are defined as

$$S=\frac{(d\sqrt{\eta_{gf}}/dt)_{t=0}}{IL}\approx\frac{\sqrt{\eta_{gf}}}{\tau_w IL} \tag{3}$$

$$M/\#=\tau_e\times\left(d\frac{\sqrt{\eta_{ef}}}{dt}\right)_{t=0}\approx\frac{\tau_e}{\tau_w}\sqrt{\eta_{ef}} \tag{4}$$

where *I* is the total writing light intensity in the two beams, *L* the crystal thickness, τ_e is the erasure time and τ_w is the writing time.

3. Results and discussion

3.1. Infrared transmission spectra

The water in the raw material and air makes the H^+ ions enter the crystal and form O–H–O during the course of crystal growing. The infrared absorption band of OH^- is near 3500 cm^{-1}. The shifting of OH^- absorption peak reflects the location and threshold concentration of the doping ions [16]. Fig. 4 shows the infrared transmission spectra of these crystals, from which it can been seen that Zr2 and Zr4 have the nearly same absorption peak positions ($\sim$at 3483 cm^{-1}) as that of Zr0, while in Zr5 the absorption peak is differently shifted to 3488 cm^{-1}.

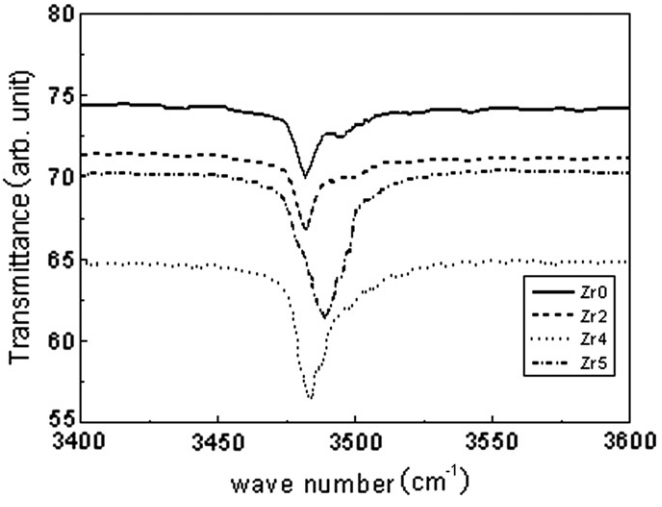

Fig. 4. Infrared absorption spectra of Zr:Fe:$LiNbO_3$ crystals.

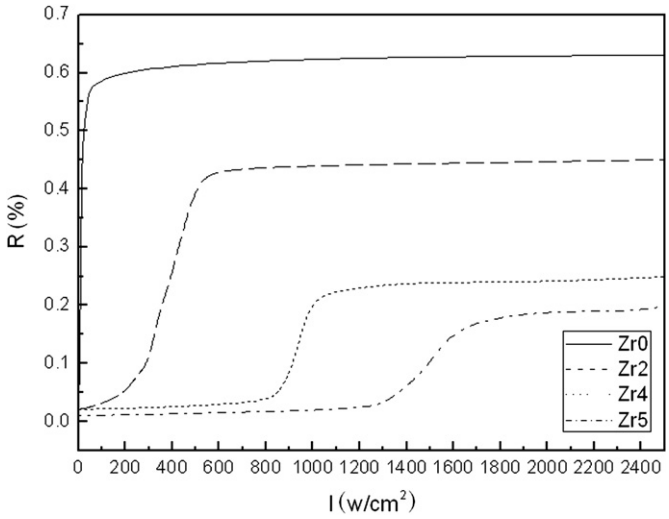

Fig. 5. Dependence of the ratio R versus the incident light intensity.

In congruent $LiNbO_3$ crystal, there always exist V_{Li}^- and Nb_{Li}^{4+} defects according to Li site vacancy model since the Li/Nb ratio in the melt is less unity. The electropositive H^+ ions are easily attracted around the electronegative V_{Li}^-. Thus the complexes $(V_{Li}^- - OH^-)$ are formed and attributed to absorption peak at 3482 cm^{-1}. In Zr2, Zr^{4+} ions replace Nb_{Li}^{4+} to normal Nb site in the form of Zr_{Li}^{3+}. In Zr4, all Nb_{Li}^{4+} disappeared, Zr^{4+} substitutes Fe_{Li}^{3+} to Nb site in the form of Zr_{Li}^{3+} and above the threshold (Zr5) Zr ions simultaneously substitute Nb sites and Li sites in the form of Zr_{Nb}^- on Nb sites. The IR absorption peaks of Zr2 and Zr4 still reflect the OH^- vibration in $(V_{Li}^- - OH^-)$ complexes and remain at the almost same position ($\sim$3483 cm^{-1}) since Zr_{Li}^{3+} defects repel H^+ ions. But in Zr5 the Zr_{Nb}^- defects may have a stronger force to attract H^+ than V_{Li}^- do, thus the H^+ ions absorb around Zr_{Nb}^- defects and form $(Zr_{Nb}^- - OH^-)$ complexes, which corresponds to the IR absorption peak of 3488 cm^{-1}.

3.2. The optical damage resistance

Fig. 5 shows the results of the ratio R depend on the incident light intensity. Threshold intensity induced by the transmitted beam scattering increases with an increase in Zr doping concentration. When the Zr doping concentration reached 5 mol% in the Zr:Fe:$LiNbO_3$ crystals, the threshold intensity was three orders of magnitude higher than that of Fe:$LiNbO_3$. Furthermore, the light scattered intensity to the high Zr doping was also much weaker than that of the Fe:$LiNbO_3$ even if the incident light intensity were over the threshold intensity. But the threshold intensity of Zr is lower than that of Mg [3].

The photorefraction σ_{ph} can be obtained to explain the experimental results of photorefractive properties [17], because it is possible to increase optical damage by increasing only photoconductivity. According to an expression, $\delta\Delta n \approx B\kappa\alpha I/(\sigma_d+\sigma_{ph})$ $(\sigma_d \ll \sigma_{ph})$, where B is the generalized electro-optical coefficient, k is the Glass constant of crystals, α is the optical absorption coefficient, I is the light intensity and σ_d and σ_{ph} are dark conductivity and photoconductivity, respectively. The σ_d is independent on the light intensity (I), may dependent on the concentration of the Li vacancies from Yan et al.'s results [8]. But in the high light intensity, the effect of σ_d to increase optical damage can be neglected.

In Zr:Fe:$LiNbO_3$, Fe ions are the most probable photorefractive centers with Fe^{3+} as electron acceptors and Fe^{2+} as electron donators. The different substitution sites of Fe^{3+} caused by Zr doping will reduce the capture across section of electrons, and enhance the photoconductivity since Fe_{Nb}^{2-} has a lower ability to trap electrons than Fe_{Li}^{3+} has [17–18]. When the doping concentration of Zr is below its threshold, Fe^{3+} ions still occupy the Li sites and do not lose their electron acceptor property. The increasing σ_{ph} is mainly attributed to the decrease in anti-site Nb_{Li}. When the concentration of Zr doping exceeds the threshold, the replacement of Fe^{3+} from in Li sites to in Nb sites induces the larger decrease in σ_{ph} since Fe_{Nb}^{2-} loses the electron acceptor properties. Consequently, the optical damage resistance ability becomes stronger. Finally, Zr begins to substitute for normal Nb ions, and the rest of Fe^{3+} on the Li sites will never decrease, so the σ_{ph} and the optical damage resistance ability remain unchanged.

Using single valence element to repel Fe_{Li}^{3+} to form Fe_{Nb}^{3+} is the most important method improving the optical damage resistance ability. Bivalency ion Mg^{2+} repelling Fe_{Li}^{3+} will form $(Mg_{Li}^{2+} - V_{Li})$ defects and tetravalent ion Zr^{4+} will form $(Zr_{Li}^{4+} - 3V_{Li})$ defects. $(Zr_{Li}^{4+} - 3V_{Li})$ defects will induce larger crystal lattice deformation than $(Mg_{Li}^{2+} - V_{Li})$ defects [19]. So we believe the abilities of repelling Fe_{Li}^{3+} of Mg are stronger than Zr. The concentration of Fe_{Li}^{3+} in Mg:Fe:$LiNbO_3$ is lower than that of Zr:Fe:$LiNbO_3$ and the threshold intensity of Zr is lower than that of Mg.

3.3. Photorefractive properties

Table 2 summarizes the photorefractive properties of these Zr:Fe:$LiNbO_3$ crystals including diffraction efficiency, response time constant, erasure time constant, photoconductivity a, photorefractive sensitivity and dynamic range. It is seen that η, τ_r and τ_e reduce with the increase in Zr doping concentration, but the drop extent is different. On the contrary, σ_{ph} and S..rises obviously. The change of $M/\#$ is irregular. Zr5 with the fastest recording speed and highest photorefractive sensitivity shows very good holographic storage property.

Table 2
Results of photorefractive properties of Zr:Fe:$LiNbO_3$ crystals.

Sample	η_{max} (%)	τ_w (s)	τ_e (s)	S (mm J^{-1})	$M/\#$	σ_{ph} (Ω^{-1} cm^{-1})
Zr0	57.5	160	475	0.78	2.25	1.77×10^{-14}
Zr2	50.8	86	203	1.33	1.68	3.29×10^{-14}
Zr4	36.6	40	148	2.52	2.23	7.08×10^{-14}
Zr5	32.5	34	128	2.79	2.14	8.32×10^{-14}

As we have discussed, Fe^{3+} ions will be pushed to Nb sites from Li site, which causes abrupt reduction of photorefractive diffraction efficiency. Increasing photoconductivity (in Table 2) indicated that motion of photo-induced charge carriers would become fast and the space charge field would form faster photorefractive response speed.

With the increase in Zr doping concentration, the maximum diffraction efficiency decreased; however, the writing and erasure time constants and photorefractive sensitivity were improved. It is believed that Zr(5 mol%):Fe:$LiNbO_3$ crystal is a promising holographic storage medium.

4. Conclusion

In summary, a series of Zr:Fe:$LiNbO_3$ crystals with varying levels of Zr doping were grown by Czochraski technique.

From the experimental results we can deduce that Zr ions initially occupied Nb_{Li}^{4+} sites and then replaced Li and Nb sites when Zr doping was up to the threshold concentration (4–5 mol%). Simultaneously, a part of Fe^{3+} ions were repelled to Nb sites from Li sites and lost their electron acceptor properties, which aroused an increase in photoconductivity. Therefore, in Zr(5 mol%):Fe:$LiNbO_3$, response time and erasure time shorten, the largest photorefractive sensitivity and the threshold intensity to optical damage was three orders of magnitude higher, in comparison with the Fe:$LiNbO_3$. Our analysis indicates that Zr(5 mol%):Fe:$LiNbO_3$ crystal is a promising holographic storage medium.

Acknowledgments

This work was supported by the National Natural Science Foundation of China (10732100).

References

[1] Furukawa Y, Sato M, Nitanda F, Ito K. Growth and characterization of MgO-doped $LiNbO_3$ for electro-optic devices. J Cryst Growth 1990;99:832.
[2] Zhang GQ, Zhang GY, Liu SM, Xu JJ, Sun Q. The threshold effect of incident light intensity for the photorefractive light-induced scattering in $LiNbO_3$:-Fe,M (M=Mg^{2+}, Zn^{2+}, In^{3+}) crystals. J Appl Phys 1998;83:4392.
[3] Jiguo Zhong, Jian Jin, Zhongkang Wu. Measurement of optically induced refractive-index damage of lithium niobate doped with different concentration of MgO. In: Proceedings of 11th international quantum electronics conference. IEEE catalog. no. 80. CH1561-0; 1980. p. 631.
[4] Volk TR, Pryalkin VI, Rubinina NM. Optical damage resistant $LiNbO_3$–Zn crystal. Opt Lett 1990;15:996.
[5] Kong YF, Wen JK, Wang HF. new doped Lithium-niobate crystal with high-resistance to photorefraction $LiNbO_3$:In. Appl Phys Lett 1995;66:280.
[6] Yamanoto JK, Kitamura K, Iyi N, Kimura S, Furukawa Y, Sato M. Increased optical-damage resistance in Sc_2O_3-doped $LiNbO_3$. Appl Phys Lett 1992;61:2156.
[7] Li S, Liu S, Kong Y, Xu J, Zhang G. Enhanced photorefractive properties of $LiNbO_3$:Fe crystals by HfO_2 codoping. Appl Phys Lett 2006;89:101126.
[8] Yan WB, Chen HJ, Shi LH, Liu SG, Kong YF. Investigations of the light-induced scattering varied with HfO_2 codoping in $LiNbO_3$:Fe crystals. Appl Phys Lett 2007;90:211108.
[9] Shi Hongxin, Sun Xiudong, Luo Suhua, Jiang Yongyuan, Meng Qingxin. Defect structure and optical damage resistance of Hf:Fe:$LiNbO_3$ crystals. Opt Laser Technol 2010;42:1118.
[10] Zhou Z, Wang B, Lin S, Li Y, Wang K. Defect structure and nonvolatile hologram storage properties in Hf:Fe:Mn:$LiNbO_3$ crystals. Optik 2011;122(13):1179–82.
[11] Kong Yongfa, Liu Shiguo, Zhao Yanjun, Liu Hongde. Highly optical damage resistant crystal: zirconium-oxide-doped lithium niobate. Appl Phys Lett 2007;91:081908.
[12] Sun Liang, Guo Fengyun, Lv Qiang, Yu Haitao. Increased optical damage resistance of Zr:$LiNbO_3$ crystals. Cryst Res Technol 2007;42:1117.
[13] Fan Yexia, Xu Chao, Xia Shixing, Guan Chengxiang, et al. Growth and spectroscopic characterization of Zr:Fe:$LiNbO_3$ crystals with various Li/Nb ratios. J Cryst Growth 2010;11:1875.
[14] Lin H, Yu B, Xu C, Luo S, Liu H, Shi H et al. Photorefractive properties of doubly doped lithium niobate crystals with Zr and Fe. In: Proceedings of SPIE—the international society for optical engineering; 2009. p. 7517.
[15] Xu C, Yang C, Mo Y, Wang Y, Sun L, Cao L, et al. Improved blue photorefractive properties of near-stoichiometric $LiNbO_3$:Mn:Fe:Zr crystal. Cryst Res Technol 2010;45:1123–6.
[16] Kovacs L, Rebout L, Soares JC, Silva MF, Hage-Ali M, Stoquert JP, et al. On the lattice site of trivalent dopants and the structure of Mg^{2+}–OH–M^{3+} defects in $LiNbO_3$:Mg crystals. J Phys Condens Mater 1993;5:781.
[17] Volk TR, Rubinina N, Wöhlecke M. Optical-damage-resistant impurities in lithium niobate. J Opt Soc Am B 1994;11:1681.
[18] Zhang T, et al. The correlation between defects and photorefractive properties in Fe:In:$LiNbO_3$ crystals. Mater Chem Phys 2007;103:137–41.
[19] Sweeney KL, Haliburton LE, Bryan DA, et al. Point defects in Mg-doped lithium nibate. J Appl Phys 1985;57:1036.